designs

MDPI

Article

On Liquid Flow Maldistribution through Investigation of Random Open-Structure Packings

Daniela Dzhonova-Atanasova *, Konstantina Stefanova and Svetoslav Nakov

Institute of Chemical Engineering, Bulgarian Academy of Sciences, "Acad. G. Bonchev" Str. Bl. 103, 1113 Sofia, Bulgaria; k.stefanova@iche.bas.bg (K.S.); s.nakov@iche.bas.bg (S.N.)
* Correspondence: dzhonova@bas.bg

Abstract: The optimal design of packed columns for separation processes is strongly dependent on an accurate prediction of the fluid flows in the packing. Insufficient knowledge about the complex factors and mechanisms governing hydrodynamic effects is compensated for by empirical information. The present study fills the gap in experimental data about the liquid phase distribution in plastic Raschig Super-Ring (RSRP) packing and plastic Ralu–Flow (RF) packing. These belong to the family of widely used random packings with an open lattice structure characterized by high mass transfer efficiency and a low pressure drop. The study was performed using the liquid collection method with a device with concentric annular collection sections at the packing outlet. Large-scale liquid maldistribution in the central and peripheral zones of the packed bed were evaluated in comparison data on competing random and structured packings. The effects of the packing size and the liquid load on the radial distribution of the superficial liquid velocity, wall flow formation and the maldistribution factor were investigated and analyzed. The results contribute to deepening the knowledge about the phenomenon of large-scale liquid flow maldistribution in packed columns, as well as to design enhancement.

Keywords: liquid flow maldistribution; liquid superficial velocity; packed bed column; random packing; wall flow

Citation: Dzhonova-Atanasova, D.; Stefanova, K.; Nakov, S. On Liquid Flow Maldistribution through Investigation of Random Open-Structure Packings. *Designs* **2023**, *7*, 47. https://doi.org/10.3390/designs7020047

Academic Editors: Luis Le Moyne and Hicham Benhayoune

Received: 5 February 2023
Revised: 26 February 2023
Accepted: 17 March 2023
Published: 24 March 2023

1. Introduction

Packed columns are typical apparatuses for separation processes in gas–liquid systems at co-current or counter-current flow. Recently, intensive research on their widespread application has been conducted in an effort to achieve a sustainable industry, as well as to reduce environmental pollution. Packed bed columns are employed for the absorption of harmful substances such as waste gases in power production and chemical industries [1]; for distillation in the production of fuels, food and pharmaceutical products; and for recovery of waste heat [2]. An important element in the design of a packed column is the choice of the type of packing, which should ensure the highest process efficiency. Lattice-type random packings are often applied in separation technologies in addition to structured packings [3]. The main advantages of these packings are high mass transfer efficiency at a low pressure drop. High performance is connected with their open-to-flow, web-like structure, which promotes turbulence, increases the interface surface area and intensifies the transfer processes. Starting in the early 1980s, leading packing manufacturers introduced a number of lattice packing elements to the market, which were initially made of plastic and, later, of ceramic and metal. A variety of models, e.g., Intalox metal tower packing (IMTP), Hiflow rings, Envipac, Fleximax, Mc–Pac, Nutter rings, Ralu–Flow and Raschig Super-Ring (RSR), can be classified as packings of the third and fourth generation [4] with moderately and highly perforated walls [3].

Lattice packings are designed on the basis of classical packing configurations, rings (Hiflow, RF), spheres (Envipac) and saddles (Super-Torus) or with entirely new configurations (RSR). An open packing structure leads to specific effects on the transport processes

in the packed bed. Updates of existing models or new models for the design of packed beds accounting for these effects have been developed. A model for the calculation of mass transfer columns was presented in [5], offering a physically grounded approach that was proven with an experimental database including over 70 types of random unperforated and lattice packings and structured packings. The authors of [3] proposed a general model for the description of mass transfer in the liquid phase for packed columns filled with random packing, including the latest generations. This approach shows the relationship between fluid dynamics and mass transfer based on a "channel model with a partly open structure" [6]. It defines three parameters characterizing the packing: the geometric surface area of the packing, the void fraction, and the form factor (the ratio of the open area to the total surface area of the packing element).

Uniform radial distribution of the phases in the packed bed is a prerequisite for maximal effectiveness of the heat and mass transfer processes in the column. Therefore, the maldistribution of flows has always been an important investigation area connected with the optimal design of packed columns. The authors of [7] presented an overview of key findings on the causes of liquid maldistribution in packed beds at the micro and macro scales, as well as the available approaches for predicting liquid spreading. The authors of [8] investigated liquid spreading without gas flow in random packings, including open-type Pall rings, as well as in structured packings. Small-scale maldistribution was registered at the scale of the packing element and explained by channeling in the column bulk, which reached a stable state called "natural flow" with a relatively low packing height [8]. Unlike large-scale non-uniformity, small-scale non-uniformity, which is the result of the discrete nature of the packing, cannot be eliminated. Large-scale maldistribution is registered at the scale of the packed bed. It is connected with the initial non-uniformity introduced by the liquid distributor and the tendency of liquid to migrate to the column wall. It was observed in [8] that the fraction of the liquid flow rate in the wall flow was smaller in structured packings than in random packings.

Radial liquid spreading has been successfully modeled by a diffusion model with various boundary conditions at the column wall [8–11]. A radial spreading coefficient is introduced in this model, which is a characteristic parameter of the packing, independent of the liquid load [8].

Liquid maldistribution is evaluated by the standard deviation of the local flow rates, which are measured over the column cross section, most often by liquid collection cells installed at the bottom of the column with different configurations, e.g., with a rectangular cross section [8], cylindrical collectors [12] or concentric annular sections [13]. Tracer methods are also employed for the investigation of radial liquid spreading [8,14].

The control of large-scale maldistribution is important in connection with scale-up problems and the trend in the industry of ever-increasing column diameters [15]. The initial uniform liquid distribution is controlled by requirements based on methods for estimation of the distributor quality. The coefficient of deviation was suggested as a criterion for distributor quality in [16]. Another method for distributor evaluation [17] considers the interaction of the liquid distributor with open-type random packings. The authors of a previous study [18] suggested a liquid distributor with dynamic control of the number and the distribution of the drip points to study the optimal initial distribution in a distillation column with a structured packing.

The wall flow increases gradually along the column wall and reaches a maximal value at equilibrium state at a certain column depth [8,19]. The equilibrium depth depends on the type and the size of the packing and is smaller at higher radial spreading coefficients. The factors that affect the wall flow are repacking, the packing type, the liquid and gas loads and the ratio of column to packing element diameter [19]. The wall flow can be controlled using technical devices, e.g., deflecting rings mounted inside the column wall [20] or liquid redistributors [21]. The latter are used to counter a possible deterioration of mass transfer efficiency along the height of the column.

The gas phase distribution is usually accepted as practically uniform if the initial distributions of the liquid and the gas phases are uniform [19]. In countercurrent flow, at higher gas flow rates, poor initial liquid distribution at the top of the column causes strong gas maldistribution due to local flooding in the top section of the bed. Initial gas non-uniformity deteriorates the liquid distribution in the bottom section of the column [19]. A strong effect of gas phase maldistribution on separation efficiency is expected in rectification systems in a concentration range of low relative volatility, as well as a large number of theoretical stages [22]. The authors of [22] proposed a method for the evaluation of the effect of small-scale vapor maldistribution on mass transfer efficiency in IMTP, RSR, and RF. The method was illustrated by the experimental results obtained for ethanol–water rectification. It was found that the effect of small-scale vapor phase maldistribution for these packings was between 14 and 38%. The gas phase distribution in open-structure packings was extensively studied in [23,24].

Numerous methods are available in the literature for the evaluation of the effect of liquid and gas maldistribution on mass transfer efficiency, e.g., methods of parallel columns [21,25] which subdivide the packed bed into several (3–100) parallel columns with different liquid–gas ratios; "by-pass" methods [26], assuming that part of the phase does not participate in the mass transfer; and methods based on computational fluid dynamics (CFD) [27]. Another approach for the prediction of mass transfer in packed columns was offered by convection–diffusion models and average–concentration models [28–31], where the velocity distribution effects were introduced by model parameters, based on experimental data. Another widely used approach is to reveal the effect of liquid distribution on local mass transfer. The authors of [32] studied the dependence between local mass transfer coefficient and liquid distribution in random Pall rings. They suggested a correlation between the overall Sherwood number across the column and the particle Reynolds number. The effect of the liquid flow pattern was investigated through a water cooling method [19,33] based on the analogy between mass and heat transfer. It was observed in [19] that for large-scale liquid maldistribution, there was a clear correlation between the liquid maldistribution factor and the temperature maldistribution factor. The higher values of the first resulted in higher values of the second. The temperature maldistribution factor appeared to be one order of magnitude less than the liquid maldistribution factor.

Investigations using experimental and theoretical techniques of liquid phase distribution in the third and fourth generation of random packings can be found in a significant number of literature sources, some of the most recent being [13,33–35]. Compared to earlier generations of packings, the latest generation packings with highly perforated walls exhibit a lower liquid spreading capacity [14]. Therefore, they are expected to retain the initial large-scale maldistribution, introduced by the liquid distributor, to a greater depth in the packing layer. They have a smaller relative wall flow and a greater packing depth for reaching maximal equilibrium wall flow than the earlier generations [36].

The latest techniques for investigation of the liquid distribution can provide a detailed picture of the flows in packed columns. They include experimental optical technologies, e.g., tomography, and numerical simulations using CFD.

Some of the most important performance characteristics of a packed column, which reflect the liquid distribution, are liquid hold-up and pressure drop. They are the focus of the research work on lattice-type packings. On the basis of the numerous acquired experimental data, a variety of equations for the prediction of these parameters is available in the literature. An example of generalization of experimental information in empirical equations is the approach used in [5], which proposed an individual relation with size-specific constants for an individual packing. Other examples are the studies conducted in [3,37], where the authors offered equations valid for a great number of packings with unperforated walls and lattice-type packings by introducing a form factor as a characteristic geometric parameter. Another approach [38] suggested equations valid for all sizes of a packing type by using as a characteristic geometric parameter the width of the lamellas of the lattice packing element.

The mechanisms of the hydrodynamic effects, such as formation and development of liquid maldistribution in the bulk and at the wall of the packed column, are still insufficiently described for the latest generations of lattice-type packings. The presented work adds to that knowledge through an experimental study of plastic packings, RSRP and RF, classified as lattice packings with moderately perforated walls, according to the form factor [3].

The aim of the present study is the investigation of the key factors influencing the liquid phase distribution in lattice-type random packings. The results are intended to provide a base for accurate prediction of the mass transfer processes and optimization of the dimensions of a packed column.

2. Materials and Methods

The presented experimental study includes measurements of the radial distribution of the liquid phase (tap water) in the absence of gas flow in a semi-industrial packed bed with a diameter D = 0.47 m and a packing layer height H = 0.6 m. The tested packings were RF 1, RF 2 (Figure 1a), RSRP 0.6 and RSRP 2 (Figure 1b). Each individual packing was successively loaded into the column and subjected to the experimental procedure.

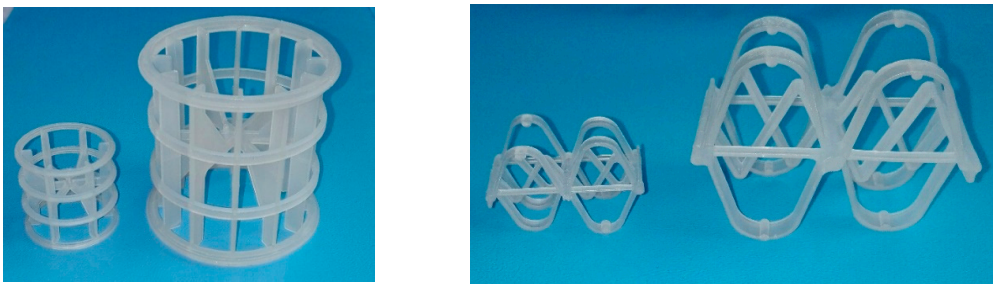

(**a**) (**b**)

Figure 1. Packings: (**a**) Ralu–Flow; (**b**) Plastic Raschig Super–Ring.

The liquid radial distribution was measured with the widely used liquid collection method. In this technique, the collector comprises a set of concentric cylinders, forming a circle in the center and concentric annuli, with equal or different cross-section surface areas. The fragmentation of the cross-section surface area of the collector determines the resolution of the obtained picture of the liquid flow. The wall flow can be measured most accurately using a special separating surface attached to the lower edge of the wall, which diverts the wall flow in an annular section with an outer diameter larger than that of the column [39]. This technique is independent of the packing size. However, in the most of the studies, including the present one, a simpler design is chosen. The wall flow is measured by selecting an empirical inner radius, smaller than that of the column, for the annular section collecting the wall flow. The proper design of the collection device is very important for obtaining correct information about the liquid distribution in the column. Different variants of possible fragmentation of the collector were estimated in [40], using dispersion model simulations for the calculation of the maldistribution factor. The effect of the fragmentation on the maldistribution factor was defined as the criterion for assessment of the collector design.

The present study used a collection device of seven concentric sections, mounted under the packing layer, as shown in Figure 2a. The local liquid flow rate in each collection section was determined by measuring the liquid volume per unit of time. The liquid collection method was applied to investigate liquid maldistribution by identifying the liquid flow rate in concentric zones of the column cross-section surface area.

The packed bed column of the experimental set-up (Figure 2) consisted of an initial liquid distribution device mounted on top of a packed bed, a liquid collection device, and a liquid tank. Tap water at room temperature was fed by a circulation pump at the top of the column in a constant level distributor tank. The liquid was spread into even jets as

it flowed through distributor drip points; then, it passed through the packing layer and reached the concentric sections of the liquid collector at the bottom of the packing bed. The local flow rate of the liquid leaving one collection section through the drain tubes was measured using the liquid volume collected in a connected measuring vessel per unit of time. The details of the experimental procedure are described in [41].

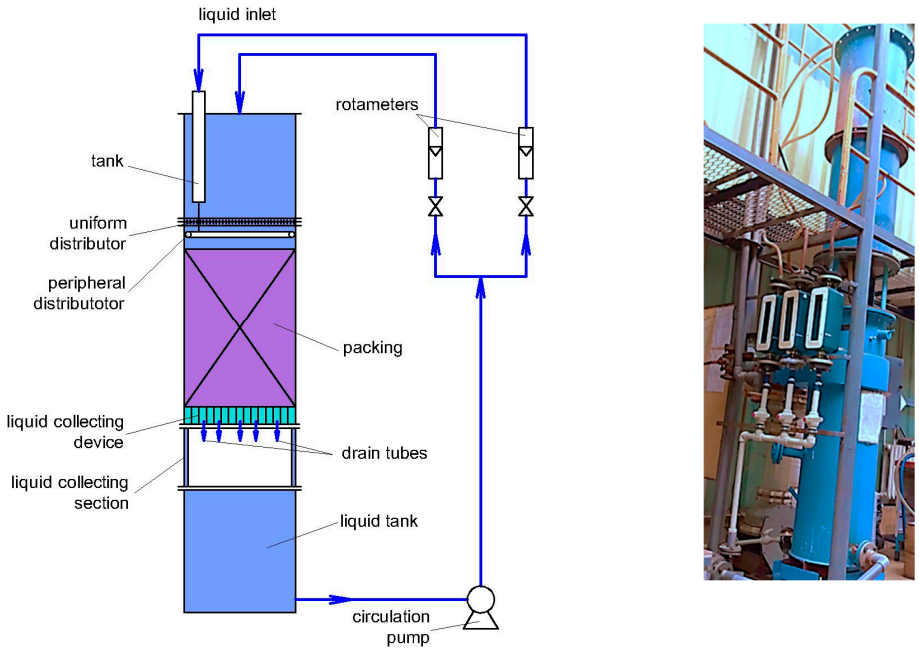

Figure 2. Semi-industrial packed column: (**a**) Scheme of the set-up; (**b**) Photography of the set-up.

Two liquid distribution devices were combined to ensure two configurations of liquid distribution: (1) uniform liquid distribution over the cross-section surface of the column and (2) peripheral distribution only on the column wall, as shown in Figure 3.

Figure 3. Photography of the uniform distributor operation.

The uniform initial distribution was provided by a shower-type liquid distributor (Figure 3) consisting of a plastic plate with Plexiglas nozzles arranged in equilateral triangles with a density of 490 drip points per m^2. To reach a wide range of liquid loads, two plates with nozzles were used. One of the plates had nozzles with a diameter of 2.5 mm and the other had nozzles with a diameter of 5.2 mm. To prevent liquid flow from the drip points directly on the column wall, the distance from the wall to the nearest peripheral points

was less than half the size of the triangle side. The uniformity of the initial distribution was checked by measuring the flow rates of the individual jets from the drip points, which showed a deviation of less than 1%. The uniformity of the jets is demonstrated by a photography showing the uniform distributor operation outside the packed bed, as shown in Figure 3.

The peripheral liquid distributor was a plastic pipe in the form of a ring with an outer diameter smaller than that of the column (Figure 3). The pipe was perforated, with a row of orifices with a diameter of 1 mm, on the pipe surface facing the column wall. They were evenly distributed 10 mm from each other.

The liquid collection device was located under the packing layer. It was divided into seven concentric sections with dimensions and cross-section surface areas presented in Table 1. The wall flow was collected in the 7th collection annulus adjacent to the column wall, which was 5 mm wide. The dimensions of the collection annuli and their drain tubes complied with the expected liquid flow rates and prevented overflow from the collector.

Table 1. Dimensions of the collection sections of the liquid collection device.

Collection Section	R_i [m]	F_i [m^2]	$\frac{F_i}{F_0}$ [%]
1	0.076	0.0181	10.5
2	0.105	0.0165	9.5
3	0.135	0.0226	13
4	0.165	0.0283	16.3
5	0.195	0.0339	19.6
6	0.230	0.0467	26.9
7	0.235	0.0730	4.2

R_i is the outer radius of a collection section i.

The measurements were performed at three liquid loads, corresponding to industrial operating conditions for rectification and absorption processes: $L_0 = 3{\cdot}10^{-3}$ m^{3}m^{-2}s^{-1}, $L_0 = 7{\cdot}10^{-3}$ m^{3}m^{-2}s^{-1} and $L_0 = 12{\cdot}10^{-3}$ m^{3}m^{-2}s^{-1}. The peripheral liquid distribution was measured at initial liquid flow rates $Q_0 = 0.35$ m^{3}h^{-1}, $Q_0 = 0.45$ m^{3}h^{-1} and $Q_0 = 0.55$ m^{3}h^{-1}.

The results are averaged from five reloadings of each packing and two runs for each reloading.

Before starting the measurements, sufficient time was provided for maximal wetting of the packing.

The liquid distribution is represented by the relative local liquid superficial velocity L_i/L_0 and the relative liquid wall flow rate Q_w/Q_0. $L_i = Q_i/F_i$ is the local liquid superficial velocity in a collection annulus i with a cross-section surface area F_i. Q_0 is the total liquid flow rate; F_0-cross-section surface area of the column; Q_i-local liquid flow rate in a collection annulus i.

A liquid maldistribution factor M_f is calculated as in the following equation [13]:

$$M_f = \frac{1}{F_0} \sum_{i=1}^{7} F_i \left| \frac{L_i - L_0}{L_0} \right| \quad (1)$$

3. Results and Discussion

The obtained data are analyzed in comparison to studies of metal Raschig Super-Ring (RSRM) (at $D = 0.47$ m and $H = 0.6$ m) with the same experimental technique [41], and data from the literature on other lattice packings and structured packings.

3.1. Uniform Initial Liquid Distribution

Figures 4 and 5 present the measured relative superficial velocity at uniform initial liquid distribution plotted versus the dimensionless radial coordinate $r = R/R_0$, where R is the radial coordinate and R_0 is the column radius. The figures show the averaged results for all liquid flow rates, packing reloadings, and measurement repetitions. The error bars

correspond to the standard deviations of all measurement values. It is observed that in the central zone of the column, at packing depth H = 0.6 m, the profiles of the liquid superficial velocity are independent of the liquid load and close to uniformity (collection sections 1–5, Table 1).

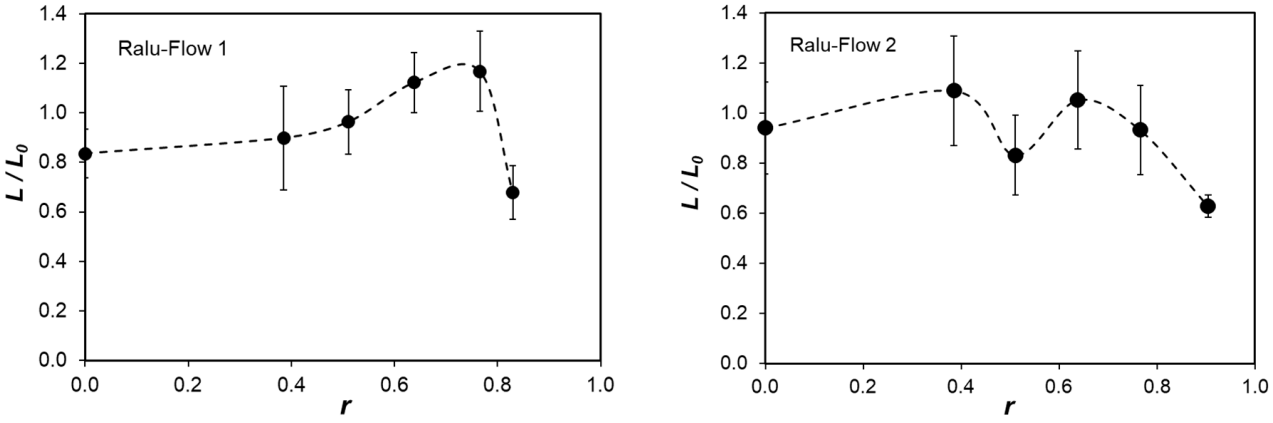

Figure 4. Relative local superficial velocity (collection sections 1–6, Table 1) in uniform initial distribution, $L_0 = 3{\cdot}10^{-3}$ $m^3m^{-2}s^{-1}$, $L_0 = 7{\cdot}10^{-3}$ $m^3m^{-2}s^{-1}$, $L_0 = 12{\cdot}10^{-3}$ $m^3m^{-2}s^{-1}$: (**a**) Ralu–Flow 1; (**b**) Ralu–Flow 2.

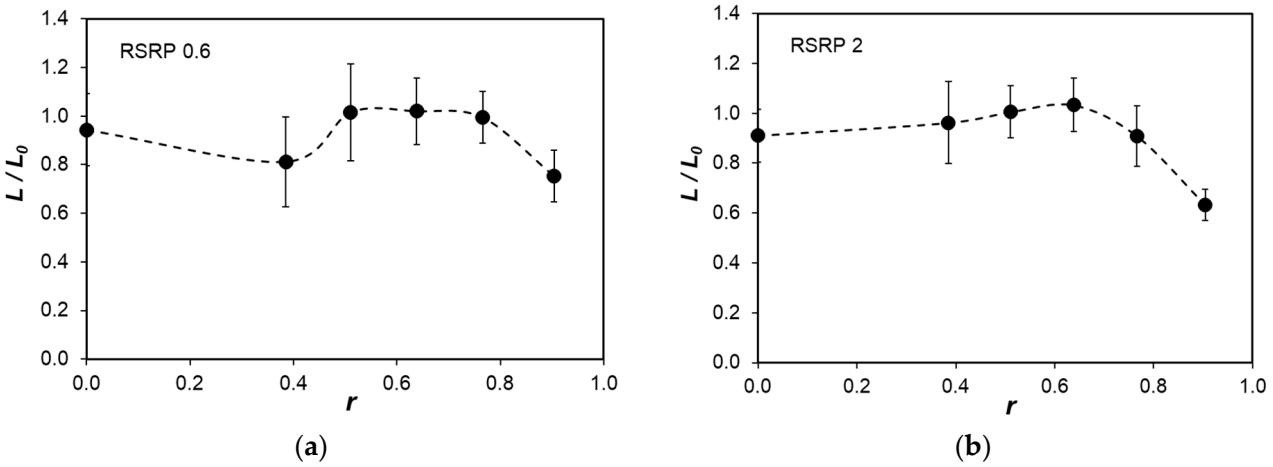

Figure 5. Relative local superficial velocity (collection sections 1–6, Table 1) in uniform initial distribution, $L_0 = 3{\cdot}10^{-3}$ $m^3m^{-2}s^{-1}$, $L_0 = 7{\cdot}10^{-3}$ $m^3m^{-2}s^{-1}$, $L_0 = 12{\cdot}10^{-3}$ $m^3m^{-2}s^{-1}$: (**a**) plastic Raschig Super–Ring 0.6; (**b**) plastic Raschig Super–Ring 2.

The largest deviation from uniformity (up to 20%) of the average superficial velocity is observed for RF (Figure 4). The deviations from the average values obtained from different liquid loads are of the same magnitude or less than those obtained from different reloadings. In the 6th collection section, the relative liquid superficial velocity decreases due to the effect of the wall flow. These observations are in agreement with the profiles of the liquid superficial velocity measured in RSRM 0.3, 1.5 and 3 [41].

The relative liquid flow rate Q_w/Q_0 in collection section 7 (Table 1) is presented in Figure 6a. The results confirm the observation in the literature that the wall flow increases with the increase in packing size, e.g., [41,42]. The data on the considered plastic packings are compared with the available data from the literature (Figure 6b) on RSRM [41] and on Sulzer 500X structured packing [12]. The relative wall flow rate decreases with the increase in the total flow rate, except for RSRP 2 and RF 2. For these packings in a small range of low liquid loads (2–5 m^3h^{-1}), the increase in the total liquid flow rate leads to the same

magnitude of the relative wall flow rate or to a small increase in it. This is in conformity with the data in the literature about other lattice-type packings, e.g., RSRM [41] (Figure 6b) and plastic Pall Rings [19]. It can be explained with the observation in [19] that at a small packing depth (below 2D), the gradient of the relative wall flow rate increases with the increase in liquid load.

It is accepted that compared to random packings, structured packings are characterized by a much better uniformity of the phases and a smaller wall flow effect [21]. The relative wall flow rate of RF 1 is the lowest (Figure 6a) and it is close to the wall flow in Sulzer 500X (Figure 6b) in an industrial distillation column for separation of Freons at total reflux with D = 0.9 m, H = 2.2 m [12].

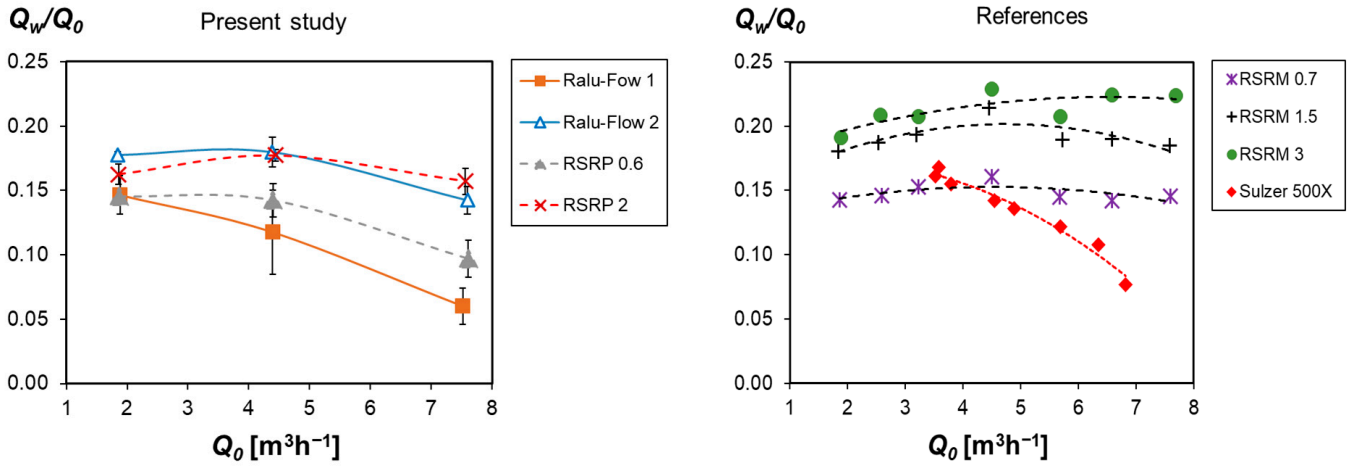

Figure 6. Relative wall flow rate in uniform initial distribution: (**a**) Present study of Ralu–Flow and plastic Raschig Super–Ring; (**b**) References: Metal Raschig Super–Ring [41] and Sulzer 500X [12].

3.2. Peripheral Initial Liquid Distribution

Figure 7 presents the relative wall flow rate in peripheral initial liquid distribution at H = 0.6 m. The measurements were performed for three values of the total liquid flow rate: Q_0 = 0.35 m^{3}h^{-1}; Q_0 = 0.45 m^{3}h^{-1} and Q_0 = 0.55 m^{3}h^{-1}. The results for RSRP 0.6, RSRP 2, RF 1 and RF 2 are compared with data about RSRM 0.7 and RSRM 3 from [41]. The results show the ability of the packings to return part of the wall flow into the bulk of the packed column. In RSRP and RSRM, the packing with bigger elements retains more liquid on the wall, while in RF, the packing with bigger elements has a smaller relative wall flow at this packing depth. This is connected with the low spreading capacity of RF 1 determined in [14]. The liquid retained in the wall flow in peripheral irrigation at 0.6 m packing depth is in the range of 75–89%, almost constant for all liquid loads. The lowest value is observed in RF 2 and the highest one in RSRM 3.

The data from this configuration of initial distribution were used for identification of the parameters in the dispersion model in [42]. In that model, the wall flow data from peripheral irrigation were used as an alternative in a lack of data about the wall flow at equilibrium state, which can be measured at a much greater packing height.

The spreading capacity of lattice packings was investigated in [14] to determine the radial spreading coefficient D_r in a diffusion model, as in Equation (2), in point source initial liquid distribution,

$$\frac{\partial L}{\partial h} = D_r\left(\frac{\partial^2 L}{\partial R^2} + \frac{1}{R}\frac{\partial L}{\partial R}\right), \quad (2)$$

where h and R are the axial and radial coordinates.

The authors of the study conducted in [14] compared a single jet technique with a tracer method using NaCl solution injected along the axis of a uniformly irrigated column. Both

techniques obtained close coefficient values for the investigated open-structure packings RSRP, RF, RSRM, IMTP. The results in [14] confirm the observations for Pall rings [8] that the spreading coefficients of packings with perforated walls are lower than those of packings with unperforated walls. Unlike the latter, the spreading coefficients of packings with perforated walls are not proportional to the nominal packing size, and for large packing elements, the spreading capacity is practically independent of the nominal size.

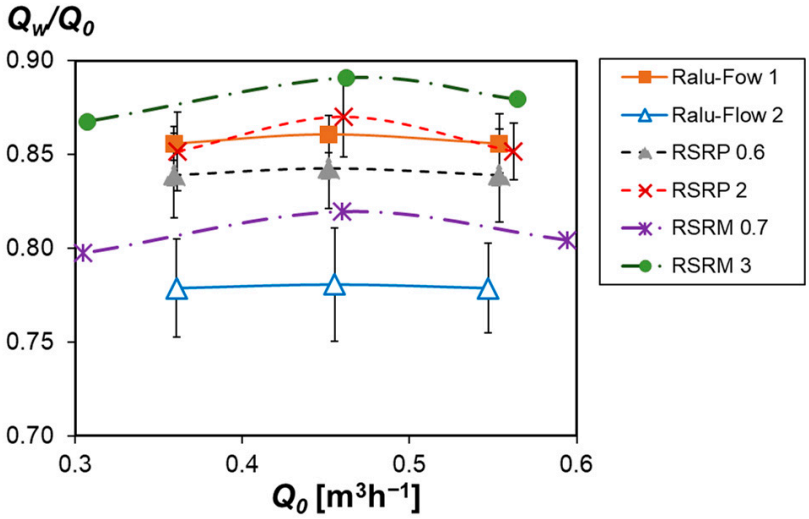

Figure 7. Average relative wall flow rate of plastic Raschig Super–Ring and Ralu–Flow in peripheral initial distribution, compared with data on metal Raschig Super–Ring [41].

3.3. Evaluation of the Liquid Radial Maldistribution

The liquid flow maldistribution of the considered packings in uniform initial distribution and H = 0.6 m, is estimated by the maldistribution factor M_f, as in Equation (1). The values of the maldistribution factor of RSRP (Figure 8a) and RF (Figure 8b) are close to the range of the values obtained in RSRM [41] (Figure 8c), as well as those obtained in Rauschert Metal Saddle Ring (RMSR) lattice packing [13] (with values in the range of 0.22–0.38 below the loading point). The RMSR packing was tested in [13] with an air–water system in a column with D = 1.2 m and H = 3 m. The operation regimes included liquid and gas loads below and above the loading point. The authors of the study summarized the most important factors affecting the liquid distribution in this type of packing as follows:

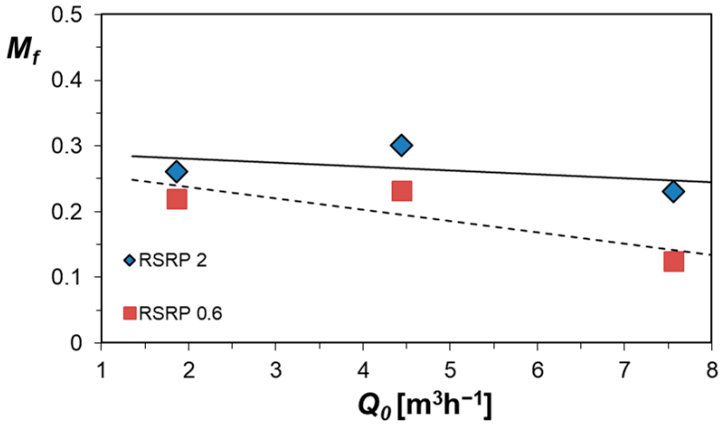

(**a**)

Figure 8. *Cont.*

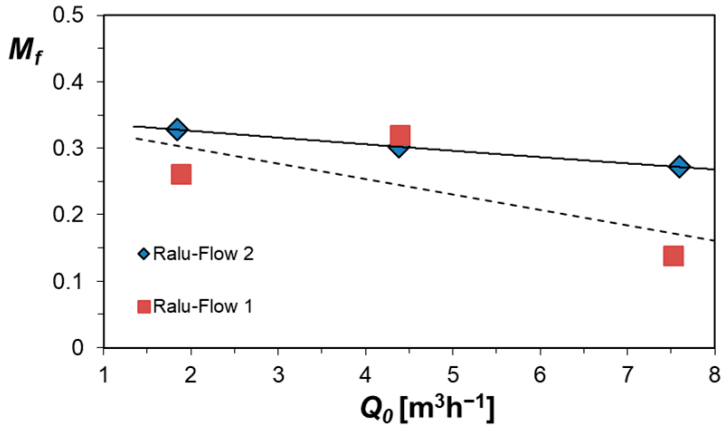

(**b**)

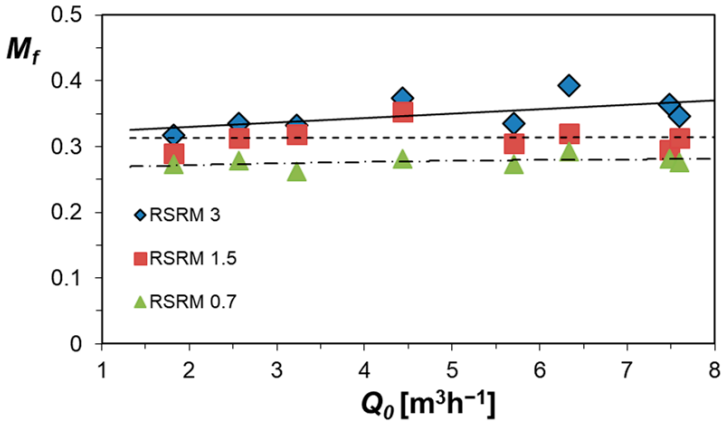

(**c**)

Figure 8. Maldistribution factor as a function of the total liquid flow rate of: (**a**) Plastic Raschig Super–Ring; (**b**) Ralu–Flow; (**c**) Reference: Metal Raschig Super–Ring [41] (with the permission of Chem. Eng. Trans.).

1. The maldistribution factor depends strongly on the liquid load and decreases with the increase in liquid load at low gas loads up to the loading point. On the contrary, at high gas loads above the loading point, the maldistribution increases with the increase in liquid load.
2. The maldistribution factor is almost independent of the gas load up to the loading point and it sharply increases with the further increase in the gas load to a maximal value in flooding conditions.
3. Below the loading point, the maldistribution slightly increases with the increase in packing height; however, after a certain height (above 2.5 m), it becomes constant and the liquid distribution assumes an equilibrium state. At gas loads above the loading point, the influence of the gas load is much stronger than that of the bed height and the data at different heights almost coincide.

The results for RSRP and RF, presented in Figure 8a,b, are in agreement with the observations mentioned above. The plots demonstrate decreasing values of the maldistribution factor with the increase in liquid load. The maldistribution factor of metal packings RSRM [41] (Figure 8c) is constant or slightly increases with the increase in liquid load, probably due to the same effect of the liquid load on the wall flow (Figure 6). In a uniform initial distribution, the formation of wall flow is the main reason for large-scale liquid maldistribution in the packing. The observation of decreasing maldistribution factor with

the increase in packing nominal size can be explained by the same relation between the wall flow and the packing size.

The comparison in [21] of maldistribution factors of several lattice-type packings with structured packings shows that with the exception of RSRM packing, all other random packings display much higher values (more than two times). The maldistribution factor of Sulzer 500X in a distillation column (D = 0.9 m, H = 2.2 m) was compared to that of RSRM (D = 0.47 m, H = 0.6 m) in [12]. The maldistribution factor of Sulzer 500X was constant and equal to 0.1 (at $3.5\ 10^{-3} < L_0 < 5\ 10^{-3}$ $m^3m^{-2}s^{-1}$and $1.3 < F_v < 2$ $Pa^{0.5}$). In these operating conditions, the countercurrent vapor flow had practically no effect on the liquid distribution and the maldistribution factor. The value of M_f of Sulzer 500X was three times higher than that of RSRM, but close to the values of RF 1 and RSRP 0.6 (Figure 8) at $Q_0 = 7.6$ m^3h^{-1} ($L_0 = 12\ 10^{-3}$ $m^3m^{-2}s^{-1}$). The further increasing of L_0 and F_v led to a substantial increase in M_f of Sulzer 500X to a value of 0.3, characteristic for RSRM [12].

4. Conclusions

The present work complements the information about the effect of different factors on liquid distribution in modern open-structure packings. New experimental data were obtained about liquid distribution in RSRP and RF. These were analyzed in combination with the available in the literature observations on large-scale maldistribution of the phases in these packings. The results can be summarized as follows:

1. In uniform initial irrigation, the liquid superficial velocity profiles in RSRP and RF are practically uniform in the column bulk and independent of the liquid load.
2. The relative wall flow in uniform initial distribution increases with the increase in nominal packing size, which leads to a higher value of the maldistribution factor. The relative wall flow and, consequently, the maldistribution factor decrease with the increase in liquid load except for a packed bed with a small height, where a small wall flow increase is observed in some packings.
3. The evaluation of the ability of the packings to return part of the wall flow in the column bulk in peripheral irrigation shows that the packings which retain more liquid in the wall flow are characterized by lower spreading capacity. The spreading capacity of the packing is independent of the liquid load and is evaluated by the spreading coefficients, calculated in point source initial distribution.
4. As expected, the large-scale liquid maldistribution in RSRP and RF is higher (M_f is two–three times higher) than in structured packings. However, there are operating conditions when M_f decreases close to the values of some structured packings.

The obtained results are intended for the development of models for precise prediction of the hydrodynamics and mass transfer with the aim of improving the design of packed columns.

Author Contributions: Conceptualization, methodology D.D.-A.; investigation K.S., D.D.-A. and S.N.; writing—original draft preparation D.D.-A.; visualization, D.D.-A. and K.S. All authors have read and agreed to the published version of the manuscript.

Funding: This research was funded by the Bulgarian Ministry of Education and Science under the National Research Program "Low-carbon energy for transport and domestic use (EPLUS)" (Agreement DO1-214/28.11.2018) and the National Program "Young scientists and postdocs-2"(DCM 206/07.04.2022).

Data Availability Statement: Please contact the corresponding author for additional research data.

Conflicts of Interest: The authors declare no conflict of interest. The funders had no role in the design of the study; in the collection, analyses, or interpretation of data; in the writing of the manuscript; or in the decision to publish the results.

Glossary

D	column diameter [m]
D_r	liquid spreading coefficient [m]
F_0	cross-section area of the column [m^2]
F_i	cross section area of the collection annulus i [m^2]
F_v	gas/vapor capacity factor [$Pa^{0.5}$]
h	axial coordinate [m]
H	height of the packing layer [m]
L_0	liquid load [$m^3m^{-2}s^{-1}$]
L_i	local liquid superficial velocity in a collection annulus i [$m^3m^{-2}s^{-1}$]
M_f	liquid maldistribution factor [–]
Q_0	total liquid flow rate [m^3h^{-1}]
Q_i	liquid flow rate in a collection annulus i [m^3h^{-1}]
$\boldsymbol{r}$	dimensionless radial cooridante, $r = R/R_0$ [–]
R	radial coordinate [m]
R_0	column radius [m]
R_i	outer radius of a collection section [m]
Abbreviations	
CFD	Computational Fluid Dynamics
IMTP	Intalox Metal Tower Packing
RF	Ralu–Flow
RMSR	Rauschert Metal Saddle Ring
RSRM	metal Raschig Super-Ring
RSRP	plastic Raschig Super-Ring

References

1. Kolev, N. *Packed Bed Columns: For Absorption, Desorption, Rectification and Direct Heat Transfer*; Elsevier: Amsterdam, The Netherlands, 2006; p. 662.
2. Darakchiev, R.; Darakchiev, S.; Dzhonova-Atanasova, D.; Nakov, S. Ceramic block packing of Honeycomb type for absorption processes and direct heat transfer. *Chem. Eng. Sci.* **2016**, *155*, 127–140. [CrossRef]
3. Mackowiak, J. Model for the prediction of liquid phase mass transfer of random packed columns for gas–liquid systems. *Chem. Eng. Res. Design* **2011**, *89*, 1308–1320. [CrossRef]
4. Schultes, M. Raschig Super-Ring. *A New Fourth Generation Packing Offers New Advantages. Chem. Eng. Res. Des.* **2003**, *81*, 48–57. [CrossRef]
5. Billet, R.; Schultes, M. Prediction of mass transfer columns with dumped and arranged packings. *Updated summary of the calculation method of Billet and Schultes. Chem. Eng. Res. Des.* **1999**, *77*, 498–504. [CrossRef]
6. Mackowiak, J. *Fluid Dynamics of Packed Columns*; Springer: Berlin/Heidelberg, Germany, 2010; p. 140.
7. Marchot, P.; Toye, D.; Crine, M.; Pelsser, A.-M.; L'Homme, L. Investigation of liquid maldistribution in packed columns by x-ray tomography. *Trans. IChemE* **1999**, *77*, 511–518. [CrossRef]
8. Hoek, P.J.; Wesselingh, J.A.; Zuiderweg, F.J. Small scale and large scale liquid maldistribution in packed columns. *Chem. Eng. Res. Design* **1986**, *64*, 431–449.
9. Cihla, Z.; Schmidt, O. A study of the flow of liquid when freely trickling over the packing in a cylindrical tower. *Collect. Czechoslov. Chem. Commun.* **1957**, *22*, 896–907. [CrossRef]
10. Staněk, V.; Kolář, V. Distribution of liquid over random packing. *Collect. Czechoslov. Chem. Commun.* **1965**, *30*, 1054–1059.
11. Porter, E.; Templeman, J. Liquid flow in packed columns. Part III: Wall flow. *Trans. Instn. Chem. Engrs.* **1968**, *46*, T86–T94.
12. Pavlenko, A.N.; Zhukov, V.E.; Sukhorukova, E.Y.; Dzhonova-Atanasova, D.B.; Stefanova, K.V. Experimental study of liquid flow maldistribution in Sulzer 500X structured packing and Raschig Super-Ring random packing. *J. Eng. Thermophys.* **2021**, *30*, 171–183. [CrossRef]
13. Hanusch, F.; Rehfeldt, S.; Klein, H. Liquid maldistribution in random packed columns: Experimental investigation of influencing factors. *Chem. Eng. Technol.* **2018**, *41*, 2241–2249. [CrossRef]
14. Dzhonova-Atanasova, D.; Kolev, N.; Nakov, S. Determination of liquid radial spreading coefficient of some highly effective packings. *Chem. Eng. Technol.* **2007**, *30*, 202–288. [CrossRef]
15. Spiegel, L. The Maldistribution Story—An Industrial Perspective. *Chem. Eng. Trans.* **2018**, *69*, 715–720. [CrossRef]
16. Zuiderweg, F.J.; Kunesh, J.G.; King, D.W. A model for the calculation of the effect of maldistribution on the efficiency of a packed column, Trans. *IChemE* **1993**, *71*, 38–44.
17. Hanusch, F.; Künzler, M.; Renner, M.; Rehfeldt, S.; Klein, H. Liquid distributor design for random packed columns. *Chem. Eng. Res. Design* **2019**, *147*, 689–698. [CrossRef]

18. Pavlenko, A.N.; Pecherkin, N.I.; Zhukov, V.E.; Meski, G.; Houghton, P. Overview of methods to control the liquid distribution in distillation columns with structured packing: Improving separation efficiency. *Renew. Sustain. Energy Rev.* **2020**, *132*, 110092. [CrossRef]
19. Kouri, R.; Sohlo, J. Liquid and gas flow patterns in random packings. *Chem. Eng. J.* **1996**, *61*, 95–105. [CrossRef]
20. Semkov, K.; Kolev, N.; Stanek, V. Theoretical and experimental investigation of the function of the wall flow deflecting ring. The determination of the optimum distance between deflecting rings. *Collect. Czechoslov. Chem. Commun.* **1987**, *52*, 2438–2446. [CrossRef]
21. Schultes, M. Influence of Liquid Redistributors on the Mass-Transfer Efficiency of Packed Columns. *Ind. Eng. Chem. Res.* **2000**, *39*, 1381–1389. [CrossRef]
22. Semkov, K.; Darakchiev, S. The influence of small scale maldistribution in the vapor phase on the efficiency of the rectification in packed columns. *Bulg. Chem. Commun.* **2010**, *42*, 194–204.
23. Darakchiev, S.; Petrova, T.; Darakchiev, R. Gas distribution in packed-bed columns with IMTP-ring and Ralu-flow. *Chem. Biochem. Eng. Q.* **2005**, *19*, 147–152.
24. Petrova, T.; Vaklieva-Bancheva, N.; Darakchiev, S.; Popov, R. Quantitative estimates of gas maldistribution and methods for their localization in absorption columns. *Clean Technol. Environ. Policy* **2014**, *16*, 1381–1392. [CrossRef]
25. Lockett, M.J.; Billingham, J.F. The Effect of Maldistribution on Separation in Packed Distillation Columns. *Trans. IChemE* **2003**, *81*, 131–135. [CrossRef]
26. Hanley, B. The influence of flow maldistribution on the performance of columns containing random packings: A model study for constant relative volatility and total reflux. *Separ. Purific. Tech.* **1999**, *16*, 7–23. [CrossRef]
27. Yin, F. Liquid Maldistribution and Mass Transfer Efficiency in Randomly Packed Distillation Columns. Ph.D. Thesis, University of Alberta, Edmonton, AB, Canada, 1999.
28. Boyadjiev, B.; Boyadjiev, C.; Popova-Krumova, P. Convective type models of co-current absorption processes in column apparatuses. *Bulg. Chem. Commun.* **2020**, *52*, 74–79.
29. Boyadjiev, C.; Doichinova, M.; Boyadjiev, B.; Popova-Krumova, P. *Modeling of Column Apparatus Processes*, 2nd ed.; Springer: Berlin/Heidelberg, Germany, 2018.
30. Chr, B.; Doichinova, M.; Boyadjiev, B.; Popova-Krumova, P. Transfer processes in industrial column apparatuses. *Math. Model.* **2017**, *1*, 23–27.
31. Boyadjiev, C.; Boyadjiev, B.; Popova-Krumova, P.; Doichinova, M. An innovative approach for adsorption column modeling. *Chem. Eng. Technol.* **2015**, *38*, 675–682. [CrossRef]
32. Dang-Vu, T.; Doan, H.D.; Lohi, A.; Zhu, Y. A new liquid distribution factor and local mass transfer coefficient in a random packed bed. *Chem. Eng. J.* **2006**, *123*, 81–91. [CrossRef]
33. Winkler, T.; Klein, H.; Rehfeldt, S. Experimental investigation of liquid maldistribution in random packed columns using temperature measurements. *Chem. Eng. Sci.* **2022**, *249*, 117350. [CrossRef]
34. Hanusch, F.; Engel, V.; Kender, R.; Rehfeldt, S.; Klein, H. Development and application of the TUM-WelChem cell model for prediction of liquid distribution in random packed columns. *Chem. Eng. Trans.* **2018**, *69*, 739–744.
35. Hanusch, F.; Kender, R.; Engel, V.; Rehfeldt, S.; Klein, H. TUM–WelChem cell model for the prediction of liquid distribution in random packed columns. *AIChE J.* **2019**, *65*, e16598. [CrossRef]
36. Boyadjiev, C.; Dzhonova-Atanasova, D.; Popova-Krumova, P.; Stefanova, K.; Pavlenko, A.; Zhukov, V.; Slesareva, E. Liquid wall flow in counter-current column apparatuses for absorption processes with random packings. *Bulg. Chem. Commun.* **2020**, *52*, 74–79.
37. Mackowiak, J. Pressure drop in irrigated packed columns. *Chem. Eng. Process.* **1991**, *29*, 93–105. [CrossRef]
38. Nakov, S.T.; Dzhonova-Atanasova, D.B.; Kolev, N.N. Pressure drop of high performance random Intalox Metal Tower Packing. *Bulg. Chem. Commun.* **2012**, *44*, 283–288.
39. Stanek, V.; Kolar, V. Distribution of liquid over a random packig. VII. The dependence of distribution parameters on the column and packing diameter. *Collect. Czechoslov. Chem. Commun.* **1973**, *38*, 1012–1026. [CrossRef]
40. Petrova, T.S.; Dzhonova-Atanasova, D.B. Simulation of the liquid distribution in the wall zone of a packed column: Case study. *Bulg. Chem. Commun.* **2019**, *51*, 91–98.
41. Dzhonova-Atanasova, D.; Petrova, T.; Semkov, K.; Darakchiev, S.; Stefanova, K.; Nakov, S.; Popov, R. Experimental investigation of liquid distribution in open structure random packings as a basis for model refinement. *Chem. Eng. Trans.* **2018**, *70*, 2077–2082. [CrossRef]
42. Petrova, T.; Semkov, K.; Dzhonova-Atanasova, D. Modeling of liquid distribution in a packed column with open-structure random packings. *Chem. Eng. Trans.* **2018**, *70*, 1051–1056. [CrossRef]